UDC: 539.23:621.383.51
Professional paper

LI-DOPED CZTS, SYNTHESIZED BY SPIN-COATING, FOR IMPROVED PV CELL PERFORMANCE

Ramadan ALITI[1,3], Yoganash PUTTHISIGAMANY[2], Mimoza RISTOVA[1*]

[1*] *Institute of Physics, Faculty of Natural Sciences and Mathematics, Ss. Cyril and Methodius University*
[2] *Solar Energy Research Institute (SERI), The National University of Malaysia*
[3] *Department of Physics, Faculty of Natural Sciences and Mathematics, University of Tetovo*
[*] *Corresponding Author: mristova@pmf.ukim.mk*

Abstract

In this work we present a comparative study of two photovoltaic cells based on n-type CZTS (Cu2ZnSnS4) kesterite-type thin films, using (a) an undoped pristine CZTS absorber and (b) doped with Li CZTS absorber, both integrated into photovoltaic (PV) cells, incorporating CdS thin film as an n-type buffer layer. The morphological, structural, compositional, optical, and electrical properties of both absorbers CZTS and CZTS:Li were studied by SEM-EDX, XRD, Vis-NIR spectroscopy, Hall-effect, and four-point probe measurements, revealing the impact on the Li-doping. The evaluation of the band gap was made using Tauc-plots. The influence of Li-doping in the CZTS films was scrutinized through the comparative study of the *IV characteristics* of PV cells. The results showed that the Li-doped CZTS yields better efficiency η=0,83% versus 0,53% for pristine CZTS absorber and better cell parameters, except for the Fill-Factor.

Keywords: CZTS, thin films, spin coating, doping, co-doping, alkali metals, sol-gel

1. Introduction

A solar cell (most known as "photovoltaics – PV") is an optoelectronic device, constructed of semiconductor material, that directly converts solar radiation into electrical energy. When solar radiation, photons reach the solar cell can be reflected, absorbed or (transmitted) pass through the cell. The operating principle of solar cells is based on (1) absorption of light by the semiconducting material and generation of pair electron-hole, (2) separation of charge carriers, and (3) extraction of charge carriers towards opposite electrodes and further to the external circuit. The total amount of current generated in the external circuit depends on the intensity and wavelength of the incident rays of the radiation. An increase in light intensity will increase the number of exited electrons in the semiconductor material, thus the current generated in the external circuit (Klaus-Dieter Jäger, Olindo Isabella, Arno H.M. Smets, René A.C.M.M. van Swaaij, Miro Zeman 2016; Sze and Lee 2012). The simplified form of the output current *I* for a solar cell, considering the series resistance *R*Sis given with (1),

$$I = I_{ph} - I_0 \left[exp\left(\frac{e(V + IR_S)}{nkT}\right) - 1 \right] \quad (1)$$

I_{ph} is photo-generated current, I_0 reverse saturation current (that depends on the optical properties of the cell, such as its ability to absorb and reflect light), e elementary charge, *k* Boltzmann constant, *T* temperature and *n* is the ideality factor used in to account for deviations from the ideal cell, reflecting the recombination losses and non-uniformities in the material. Other important quantities for the characterization of PV cells are short circuit current (I_{sc}) and open-circuit voltage (V_{oc}). The short circuit current (I_{sc}), that is used to describe the maximum current (photocurrent) that a solar cell can deliver that can be obtained for bias *V=0* (Solanki

https://doi.org/10.62792/ut.jnsm.v9.i17-18.p2846

2015; Mertens and Roth 2014; Klaus-Dieter Jäger, Olindo Isabella, Arno H.M. Smets, René A.C.M.M. van *Swaaij, Miro Zeman 2016),*

$$I_{SC} = I_{ph} - I_0\left(e^{\frac{e\cdot 0}{nkT}} - 1\right) = I_{ph} \tag{2}$$

While V_{oc} is the maximum voltage that a solar cell can deliver, occurring when no current flows through the external circuit. V_{oc} corresponds to the forward bias voltage at of the *p-n* junction due to the light-generated current. Practically, it is a measure of the recombination in the solar cell, so it depends on the photo-generated current density and can be calculated from Equation (3) (Solanki 2015; Mertens and Roth 2014; Klaus-Dieter Jäger, Olindo Isabella, Arno H.M. Smets, René A.C.M.M. van Swaaij, Miro Zeman 2016),

$$V_{OC} = \frac{nkT}{e}\ln\left(\frac{J_{ph}}{J_0} + 1\right) \tag{3}$$

This equation illustrates that V_{oc} depends on the saturation current density (J_0) of the solar cell and the photo-generated current (J_{ph}). While Jph usually varies slightly, the saturation current can vary significantly. The J_0 is affected by recombination in the solar cell. Thus, the V_{oc} deficiency (which is presented by its deviation from the theoretical boundary (Shockley Queiser limit) serves as an indicator of the recombination level in the device.

In order to optimize the operation of the solar cells (or PV modules) a concept of fill factor (*FF)* is also used. *FF* is defined as the ratio between the maximum power point ($P_{max} = J_m\ V_m$) generated by a solar cell and the product of J_{sc} with V_{oc}, Equation (4) (Solanki 2015; Mertens and Roth 2014; Klaus-Dieter Jäger, Olindo Isabella, Arno H.M. Smets, René A.C.M.M. van Swaaij, Miro Zeman 2016),

$$FF = \frac{J_m \cdot V_m}{J_{SC} \cdot V_{OC}}. \tag{4}$$

The conversion efficiency of a solar cell is calculated as the ratio between the maximum power (P_{max}) it can generate, and the incident power (P_{in}) it receives. In testing, the incident power is typically standardized to the irradiance of the AM1.5 spectrum, which is equivalent to 1 kW/m². The efficiency can be alternatively defined as a function of the fill factor (*FF*), short-circuit current (I_{sc}), and open-circuit voltage (V_{sc}), divided by the incident power (power input) - P_{in}, Equation (5) (Solanki 2015; Mertens and Roth 2014; Klaus-Dieter Jäger, Olindo Isabella, Arno H.M. Smets, René A.C.M.M. van Swaaij, Miro Zeman 2016),

$$\eta = \frac{P_{max}}{P_{in}} = \frac{Jsc \cdot Voc \cdot FF}{P_{in}} \tag{5}$$

The *IV* characteristic of a solar cell represents the dependence of the current on the voltage change, a curve showing its operating parameters based on its equivalent circuit. The IV characteristic of a solar cell is a superposition of IV curves in dark and light conditions (Solanki 2015; Mertens and Roth 2014; Klaus-Dieter Jäger, Olindo Isabella, Arno H.M. Smets, René A.C.M.M. van Swaaij, Miro Zeman 2016).

Each of the PV cell layers and interfaces exhibits specific defects affecting the open-circuit voltage (V_{oc}), short-circuit current density (I_{sc}) and the fill factor (*FF*), thus limiting the achievement of maximum performance of the solar cells. The theoretical maximum efficiency of CZTS-based solar cells stands at 32.2%. However, practical accomplishments reported efficiencies up to 13.6% (Gong et al. 2021). This disparity is attributed to unresolved challenges, such as stoichiometry control, surface defects, interface quality, creation of sulfur vacancies,

and others. Beside their complexity of defects and electronic structure, quaternary systems are providing opportunities for material optimization by control of compositional gradients and stoichiometry (He et al. 2021; Pal et al. 2019; Siebentritt 2013).
Overcoming these challenges requires further research, such as optimization of the deposition process, precursor chemistry, sulfurization methods, and post-deposition treatments. To optimize the photovoltaic properties, various improvement strategies for CZTS absorber are provided, including the doping with Lithium (Li) has been considered in many studies (Wang et al. 2018; Shen et al. 2021). Li doping can have several effects on the structural, optical, and electrical properties of CZTS, which can ultimately influence the performance of CZTS-based solar cells. Based on Romanyuk *et al.* (Romanyuk et al. 2019), due to the ionic radius of Li+ (0.73 *Å*) being very close to that of Cu+ (0.74 *Å*), Li has the highest probability of being incorporated into the lattice of the kesterite phase, which can significantly affect the photovoltaic properties of CZTS. Wang *et al.* (Wang et al. 2018) in 2018 reported that "lithium doping was found to promote kesterite grain growth and minimize interface charge recombination opening new prospects for kesterite photovoltaics". Similar to Shen *et al.* (Shen et al. 2021) for CZTSe, Muska *et al.* (Muska et al. 2023) showed that the addition of Li into CZTS absorber mostly affected the V_{OC} value. Based on the above, the device architecture of the two PV-cells engineered for the merits of comparative study for examination of the effect of Li-doping in CZTS on cell parameters, is as follows:

(1) PV cell based on Undoped CZTS, Mo/CZTS:Li/CdS/i-ZnO/ITO/Ag and
(2) PV cell based on Li-doped CZTS, Mo/CZTS/CdS/i-ZnO/ITO/Ag.

2. Materials and methods

The absorbers of the two cells described above are made of the undoped CZTS (UnD) and Li-doped CZTS (LiD) thin films, deposited by spin coating on sodium lime glass (SLG) substrates. The samples were characterized by examination of their: (a) morphology and quantitative analysis, using field emission scanning electron microscopy (FESEM-DX), and (b) crystallography by examination of their XRD patterns, recorded by Bruker AXS-D8 advance system equipped with a Cu-Kα source (λ =1.5406 Å) for 2 Theta angles between 15° to 60°. Optical transmittance spectra were recorded by UV/VIS/NIR Spectrometer (PerkinElmer Lambda 950) instrument. The bang gap was evaluated by using Tauc plot and the following Equation (6).

$$\alpha h\nu = C\left(h\nu - E_g\right)^{1/n} \tag{6}$$

where *h* is the Planck constant, *hν* is the energy (in eV) of the incident photons, *n* is a constant related to the band structure (where for direct bandgap semiconductors *n*=2). In this way, by extrapolating the linear part of the curve, $(\alpha h\nu)^2$ for the photon energy, we can also estimate the bandgap energy of the semiconductor. For electrical properties of the samples, such as mobility, carrier concentration, and resistivity four-point probe (Ossila) and Hall effect measurement system (ECOPIA HMS-2000) 0.57 T at 300 K were employed.
The cell design (architecture) is depicted in Figure 1. Herein the substrate is made of sodium lime glass. The back-contact is composed of Mo-layer, approximately 100-1000 nm thick. This is because Mo establishes ohmic contact with the subsequent layer (CZTS absorber), reduces recombination, and helps the rapid passage of minority carriers to reach the *n*-type material (buffer layer) used in the solar cell (Pandharkar et al. 2018). The absorber layer is composed of spin-coated *p*-type CZTS (either doped with Li (LiD) or undoped (UnD) of approximately 1000-2000 nm (Swami et al. 2013; Yu et al. 2014). The buffer layer is an *n*-type CdS film prepared by chemical bath deposition (CBD) technique of about 30-150 nm thick (Azmi et al. 2020). At the interface of CZTS/CdS, a *p-n* heterojunction is formed. The window layer is

composed of RF-sputtered multilayered wide gap transparent semiconductors of Indium Tin Oxide (ITO) and another thinner layer of intrinsic zinc oxide (i-ZnO) 10-80 nm thick, was introduced to passivate defects, reduce recombination of charge carriers, and enhance the efficiency of the solar cell (Nugroho et al. 2022). Front contact is made of DC-sputtered Ag grid shape (fishbone of comb) using a mask.

The *IV* characteristics of the samples shown in Figure 2, were recorded using *IV* tester. The tester has undergone a calibration process (to replicate the standard 1.5 AMG spectrum, which is made possible by the adjustable intensity of the halogen arc lamp attached to the *IV* tester) according to the specified standards of the National Renewable Energy Laboratory (NREL), where the obtained value of J_{sc} is compared with J_{sc} results supplied by the NREL.

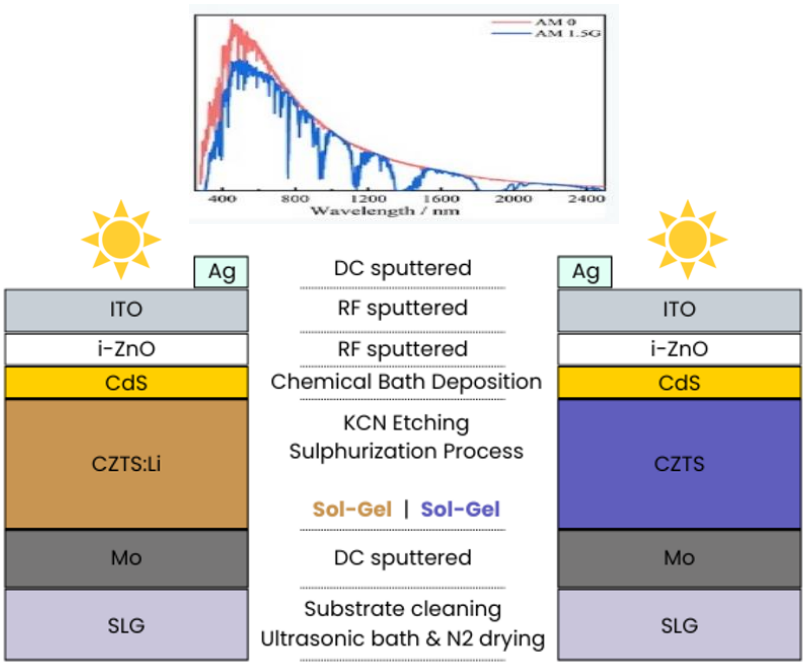

Figure 1. Complete fabrication process of CZTS doped and undoped solar cells - the structure of CZTS based solar cells: (left) CZTS doped with Li, (right) CZTS undoped. Solar spectra AM1 and AM1.5G (Mertens and Roth 2014)

Figure 2. Two PV-cells, incorporating undoped CZTS and CZTS:Li absorbers, with front Ag-electrodes (fishbone-grid).

3. Results and discussion

FESEM images of undoped (UnD) and Li doped (DLi) presented at Figure 3 show obvious differences in their morphology. The surfaces of both samples reveal pronounced porosity, probably due to the rapid evaporation process (especially in the UnD sample). The elemental atomic composition of the CZTS absorbers are presented in Table 1. The atomic composition of the undoped CZTS sample, UnD suggests a slightly Cu-rich composition (Cu/Sn > 3), indicating excess of copper in the crystal structure, while as maintaining a relatively balanced S/metal ratio close to 1, indicating a near-stoichiometric CZTS film. However, the Cu/Sn ratio for the DLi samples drops to values between 2.29.

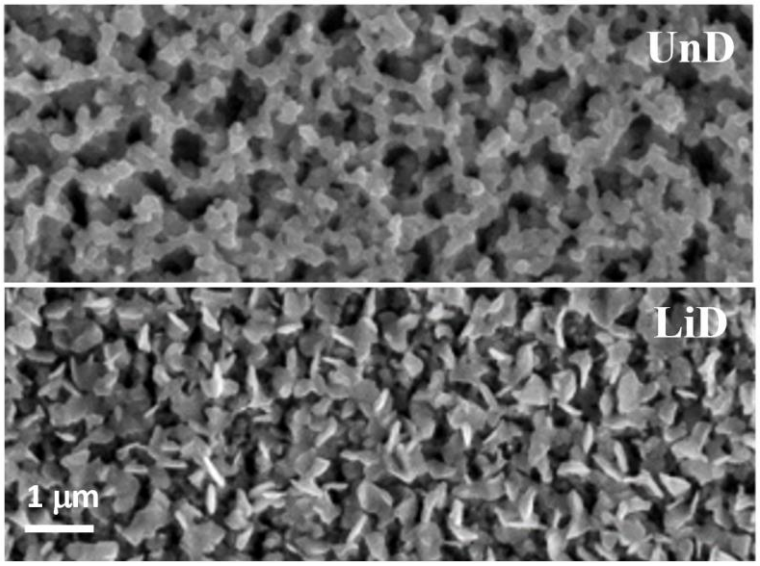

Figure 3. SEM images for the CZTS absorber on Mo-coated glass: (top) undoped (UnD) and (bottom) doped with Li (LiD).

The S/metal ratio for both samples is relatively close to stoichiometric values, suggesting that doping process did not interfere with the CZTS stoichiometry. Due to the Sn evaporation during the annealing process, observations shows that the expected Cu-poor composition with (Cu/Sn) < 2 and (Cu/(Zn+Sn)) < 0.9, and a Zn-rich composition with (Zn/Sn) > 1 has not been achieved (He et al. 2021; Pal et al. 2019).

Table 1. Elemental composition (in at%) and their ratio of CZTS films measured with FESEM-EDX. The elemental content of the Li-dopant is below the detection limit at the given conditions.

Sample	S, at%	Cu, at%	Zn, at%	Sn, at%	Cu/Sn	Cu/(Zn+Sn)	Zn/Sn	S/(Cu+Zn+Sn)
UnD	47.8	30.1	12.3	9.8	3.07	1.36	1.26	0.92
DLi	46.4	27.5	14.1	12	2.29	1.05	1.18	0.87

The XRD patterns, presented in Figure 3, for UnD-CZTS and DLi-CZTS samples, suggest polycrystalline films with diffraction peaks from (101), (112), (103), (200), (220), (312) and (116) planes characteristic for both the tetragonal kesterite CZTS crystal phases (JCPDS 26-0575) (Ito 2015; Scragg 2011; Kattan et al. 2015). Also, there are two peaks originating from the molybdenum (Mo) substrate layer at $2\theta = 40.6°$ and 73.8°. The 2θ values for the most intense peak originating from (112) plane are observed in the narrow range between 28.5° and 28.6°. This suggests a preferred crystal orientation along (112) plane for both samples.
Influencing their optical properties, doping process of CZTS thin films, alters their band gap. Using the transmittance spectra and the Tauc-plot shown in Figure 4 (a) and (b), the band gap

(E_g) of both samples was evaluated. E_g was evaluated from the intercept of the extrapolated linear regression model applied on the $(Ahv)^2$ versus photon energy plot, where A is the absorbance of the film, calculated from the film transmittance (T), h is Planck's constant and v is the incident photon frequency. The results show that the bandgap value of the Li doped film, DLi (1.36 eV) is red-shifted in comparison to the UnD (1.39 eV), suggesting that Li doping influenced the optical properties of CZTS (Romanyuk et al. 2019; Muska et al. 2023) . This reduction is in-line with with the findings of many researchers, that the doping with alkali metals enhancing the CZTS suitability for light absorption. The Hall effect measurements, presented on Table 2 were conducted to explore the transport parameters and the carrier concentration of the samples. The results of the calculated carrier transport parameters from the Hall effect measurements indicated predominantly *p*-type behavior for DLi films, while the UnD sample in certain random measurements exhibited n-type behavior. The Hall effect measurements, presented on Table 2 were conducted to explore the transport parameters and the carrier concentration of the samples. The results of the calculated carrier transport parameters from the Hall effect measurements indicated predominantly *p*-type behavior for DLi films, while the UnD sample in certain random measurements exhibited n-type behavior.

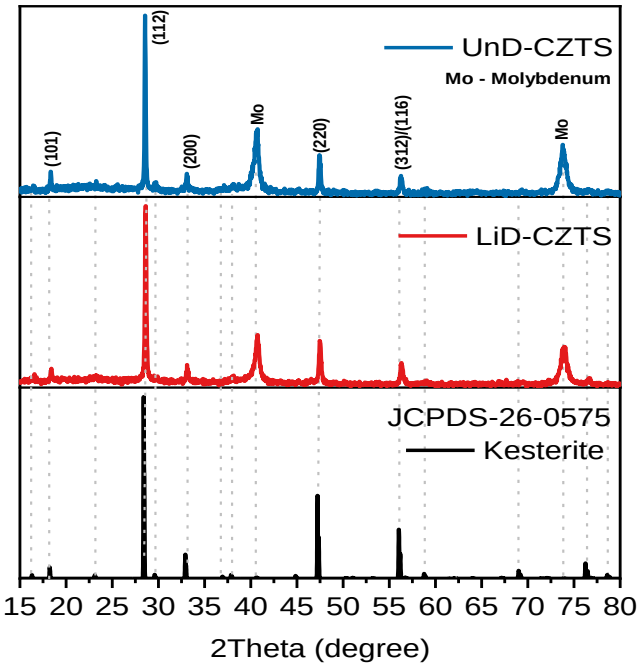

Figure 3. XRD of UnD and LiD CZTS on Mo-coated glass, in comparison to kesterite file JCPDS-26-0575.

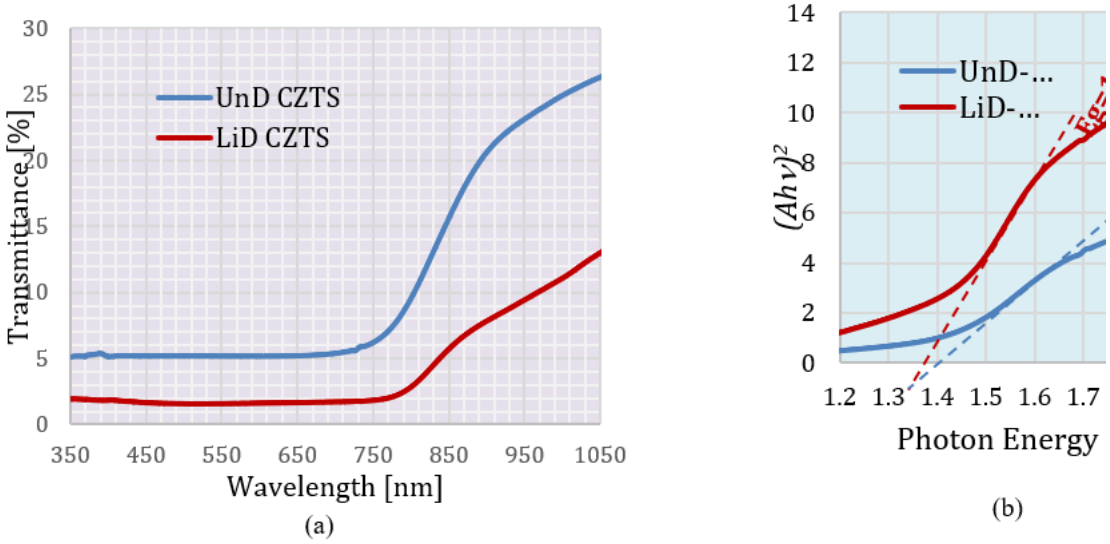

Figure 4. (a) Transmittance spectra of UnD CZTS and LiD CZTS, and (b) corresponding Tauc-plots asuming direct transition and bang gap (E_g) evaluation.

The doping was found to decrease the film resistivity (ρ) from 1.33×10^4 m to 1.32×10^4 m for the Li doped CZTS films. The carrier mobility (μ) of the undoped CZTS (UnD) sample was found to be 11.17 cm^2/Vs, and increased for the DLi sample to 20.14 cm^2/Vs. The sheet resistance of the samples was explored with the four-point probes technique showed that doping process decrease the sheet resistance from 110.86 kΩ/☐ for UnD to 67.895 kΩ/☐ for Li doped sample DLi (Muska et al. 2023; Yan et al. 2022).

Table 2. Electrical properties of the undoped and Li-doped CZTS kesterite type, and resistivity (ρ), carrier concertation (N), mobility (μ), Hall coefficient (R_H) and sheet resistance (R_S)

Sample	Type	ρ (Ωcm)	N ($1/cm^3$)	μ (cm^2/Vs)	R_S (kΩ/☐)	Reference
UnD	n-p	1.33×10^4	4.77×10^{13}	11.17	110.86	[17]
DLi	p	1.32×10^4	11.22×10^{13}	20.14	67.95	[22]

Analyzing the *IV* characteristics of the two types of solar cells, one with undoped CZTS and the other with Li (CZTS:Li), provides crucial insights into their performance. The results of these measurements are presented as current-voltage (*IV*) curves with an annotation of maximum power point (*MPP*) voltage (V_{max}) and current (I_{max}) values, as shown in Figure 5 and supported by the data in Table 3, reveal essential parameters of the solar cells. Herein, the efficiency of the CZTS:Li PV cell is calculated to be 0.85%, much higher than for the undoped CZTS (0.52%) (Yan et al. 2022; Muska et al. 2023). It is also evident that the CZTS:Li cell demonstrated a better PV performance through the lower serial resistance (R_s = 97.67 Ω) compared with the cell based on undoped CZTS (R_s = 113.65 Ω). Also, the short circuit current is about double higher for the Li-doped sample (I_{sc} =1.60 mA versus 0.81 mA). Moreover, there is a substantial increase of the Fill Factor due to the Li-doping (FF = 0.47 versus 0.37).

Finally, the insufficient efficiency and competitiveness of the PV performance of the Li-doped CZTS, subject to this study, compared to the champion cells reported by other authors, could be ascribed to the considerable shunt resistance (R_{sh}), which affects the leakage current paths in the solar cell, and the ideality factor (a), which affects the cell's current-voltage characteristics. Given the complex structure, other possible factors include the quality of the absorber and semiconductor contacts, and interface recombination. Further investigation into these factors is essential for a comprehensive understanding of their impact on solar cell performance.

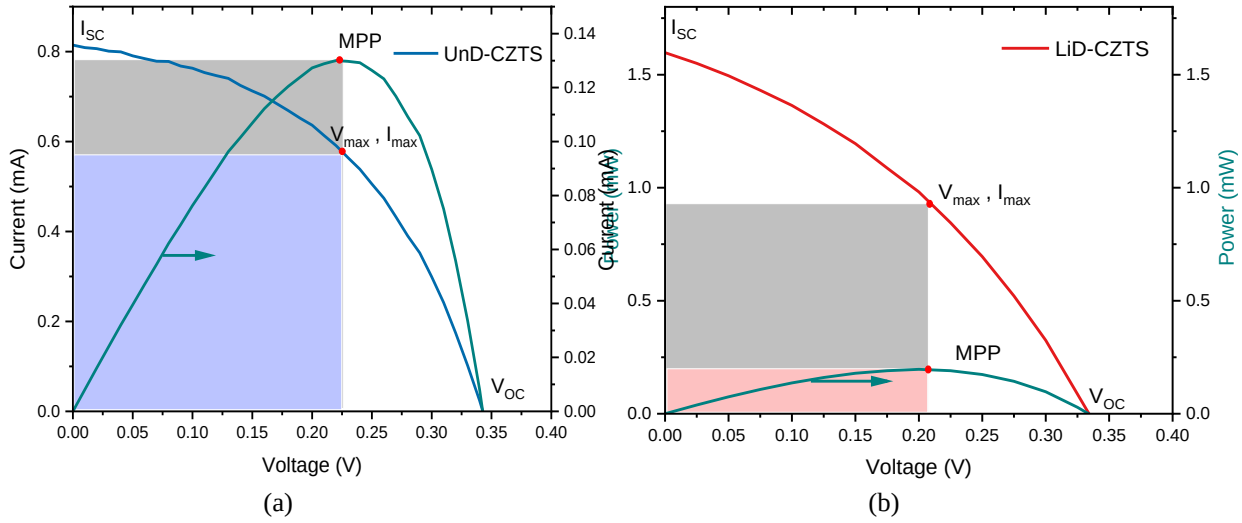

Figure 5. IV curves of (a) Undoped CZTS and (b) Li doped CZTS solar cell.

Table 3. CZTS and CZTS: Li cell parameters

Parameters	**CZTS**	**CZTS:Li**
I_{sc} **(mA)**	0.81	1.60
J_{sc} **(mA/cm^2)**	3.26	6.95
V_{oc} **(V)**	0.34	0.33
***FF*- Fill Factor**	0.47	0.37
Efficiency (%)	0.52	0.85
P_{max} **(mW)**	0.13	0.20
I_{max} **(mA)**	0.57	0.94
V_{max} **(V)**	0.23	0.21
R_s **(Ω)**	113.65	97.67

4. Conclusions

In this research, two solar cells were fabricated using undoped CZTS and Li-doped CZTS as the *p*-type semiconductor and CdS as the *n*-type semiconductor. The CZTS absorber layer was synthesized using the spin coating sol-gel method on Mo-coated glass substrates from fluoride precursor of the corresponding metals.

The CdS layer was deposited by chemical bath deposition. The back electrodes were designed using Ag grade and deposited using DC sputtering. *IV* characteristics were recorded under normal illumination of the PV cells with an AM1.5 solar spectrum simulator. The obvious cell parameter improvement was achieved with the Li-doped solar cell (CZTS:Li), showing V_{OC} = 0.33 *V*, I_{sc} = 1.59 *mA*, *FF* = 0.37, and η = 0.85%. These results were compared to those of the undoped CZTS, revealing that the CZTS:Li cell exhibited considerably higher power efficiency than the undoped CZTS (0.52%).

References

[1] Azmi, N.; Chelvanathan, P.; Yusoff, Y.; Shahahmadi, S. A.; Tiong, S. K.; Sopian, K.; Amin, N. (2020): A comprehensive study on the effects of alternative sulphur precursor on the material properties of chemical bath deposited CdS thin films. In *Ceramics International* 46 (11), pp. 18716–18724. DOI: 10.1016/j.ceramint.2020.04.186.

[2] Gong, Yuancai; Zhang, Yifan; Jedlicka, Erin; Giridharagopal, Rajiv; Clark, James A.; Yan, Weibo et al. (2021): Sn4+ precursor enables 12.4% efficient kesterite solar cell from DMSO solution with open circuit voltage deficit below 0.30 V. In *Sci. China Mater.* 64 (1), pp. 52–60. DOI: 10.1007/s40843-020-1408-x.

[3] He, Mingrui; Yan, Chang; Li, Jianjun; Suryawanshi, Mahesh P.; Kim, Jinhyeok; Green, Martin A.; Hao, Xiaojing (2021): Kesterite Solar Cells: Insights into Current Strategies and Challenges. In *Advanced science (Weinheim, Baden-Wurttemberg, Germany)* 8 (9), p. 2004313. DOI: 10.1002/advs.202004313.
[4] Ito, K. (2015): Copper zinc tin sulphide-based thin-film solar cells. Chichester: Wiley-Blackwell.
[5] Kattan, Nessrin; Hou, Bo; Fermín, David J.; Cherns, David (2015): Crystal structure and defects visualization of Cu2ZnSnS4 nanoparticles employing transmission electron microscopy and electron diffraction. In *Applied Materials Today* 1 (1), pp. 52–59. DOI: 10.1016/j.apmt.2015.08.004.
[6] Klaus-Dieter Jäger, Olindo Isabella, Arno H.M. Smets, René A.C.M.M. van Swaaij, Miro Zeman (2016): Solar energy: fundamentals, technology and systems.
[7] Mertens, Konrad; Roth, Gunther (2014): Photovoltaics. Fundamentals, technology and practice / Konrad Mertens ; translated by Gunther Roth. Chichester, West Sussex: Wiley.
[8] Muska, Katri; Timmo, Kristi; Pilvet, Maris; Kaupmees, Reelika; Raadik, Taavi; Mikli, Valdek et al. (2023): Impact of Li and K co-doping on the optoelectronic properties of CZTS monograin powder. In *Solar Energy Materials and Solar Cells* 252, p. 112182. DOI: 10.1016/j.solmat.2023.112182.
[9] Nugroho, Harbi Setyo; Refantero, Gema; Septiani, Ni Luh Wulan; Iqbal, Muhammad; Marno, Septhian; Abdullah, Huda et al. (2022): A progress review on the modification of CZTS(e)-based thin-film solar cells. In *Journal of Industrial and Engineering Chemistry* 105, pp. 83–110. DOI: 10.1016/j.jiec.2021.09.010.
[10] Pal, Krishan; Singh, Pawan; Bhaduri, Abhishikta; Thapa, Khem B. (2019): Current challenges and future prospects for a highly efficient (>20%) kesterite CZTS solar cell: A review. In *Solar Energy Materials and Solar Cells* 196, pp. 138–156. DOI: 10.1016/j.solmat.2019.03.001.
[11] Pandharkar, Subhash M.; Rondiya, Sachin R.; Rokade, Avinash V.; Gabhale, Bharat B.; Pathan, Habib M.; Jadkar, Sandesh R. (2018): Synthesis and Characterization of Molybdenum Back Contact Using Direct Current-Magnetron Sputtering for Thin Film Solar Cells. In *Front. Mater.* 5, Article 13. DOI: 10.3389/fmats.2018.00013.
[12] Romanyuk, Yaroslav E.; Haass, Stefan G.; Giraldo, Sergio; Placidi, Marcel; Tiwari, Devendra; Fermin, David J. et al. (2019): Doping and alloying of kesterites. In *J. Phys. Energy* 1 (4), p. 44004. DOI: 10.1088/2515-7655/ab23bc.
[13] Scragg, Jonathan J. (2011): Copper Zinc Tin Sulfide Thin Films for Photovoltaics. Synthesis and Characterisation by Electrochemical Methods. Berlin, Heidelberg: Springer Berlin Heidelberg.
[14] Shen, Zhan; Wang, Siyu; Liu, Yue; Sun, Yali; Wu, Jianyu; Guo, Hongling et al. (2021): Li2S doping into CZTSe drives the large improvement of VOC of solar cell. In *Journal of Energy Chemistry* 62, pp. 637–644. DOI: 10.1016/j.jechem.2021.04.018.
[15] Siebentritt, Susanne (2013): Why are kesterite solar cells not 20% efficient? In *Thin Solid Films* 535, pp. 1–4. DOI: 10.1016/j.tsf.2012.12.089.
[16] Solanki, Chetan Singh (2015): Solar photovoltaics. Fundamentals, technologies and applications. Third edition. Delhi: PHI Learning Private Limited.
[17] Swami, Sanjay Kumar; Kumar, Anuj; Dutta, Viresh (2013): Deposition of Kesterite Cu2ZnSnS4 (CZTS) Thin Films by Spin Coating Technique for Solar Cell Application. In *Energy Procedia* 33, pp. 198–202. DOI: 10.1016/j.egypro.2013.05.058.
[18] Sze, S. M.; Lee, M. K. (2012): Semiconductor devices, physics and technology. 3rd ed. Hoboken N.J.: Wiley.
[19] Wang, Zhuoran; Brodusch, Nicolas; Gauvin, Raynald; Demopoulos, George P. (2018): Lithium-doped Cu2ZnSnS4 superstrate solar cells with 5% efficiency – An alternative to thin film kesterite photovoltaics. In *Nano Energy* 53, pp. 130–134. DOI: 10.1016/j.nanoen.2018.08.049.
[20] Yan, Qiong; Sun, Quanzhen; Deng, Hui; Xie, Weihao; Zhang, Caixia; Wu, Jionghua et al. (2022): Enhancing carrier transport in flexible CZTSSe solar cells via doping Li strategy. In *Journal of Energy Chemistry* 75, pp. 8–15. DOI: 10.1016/j.jechem.2022.07.031.
[21] Yu, Yue; Ge, Jie; Prabhakar, Tejas; Yan, Yanfa (2014): Effects of spin speed on the properties of spin-coated Cu2ZnSnS4 thin films and solar cells based on DMSO solution. In : 2014 IEEE 40th Photovoltaic Specialist Conference (PVSC). 2014 IEEE 40th Photovoltaic Specialists Conference (PVSC). Denver, CO, USA, 6/8/2014 - 6/13/2014: IEEE, pp. 448–451.